Cement and Concrete Research 40 (2010) 179–188

Contents lists available at ScienceDirect

Cement and Concrete Research

journal homepage: http://ees.elsevier.com/CEMCON/default.asp

# Changes in $C_3S$ hydration in the presence of cellulose ethers

J. Pourchez [a,*], P. Grosseau [a], B. Ruot [b]

[a] Ecole Nationale Supérieure des Mines de Saint-Étienne (ENSMSE), LPMG: Process in Granular Media Laboratory CNRS UMR 5148, 158, cours Fauriel 42023 Saint-Étienne Cedex 2, France
[b] Scientific and Technical Centre for Building (CSTB), 24, rue Joseph Fourier, 38400 Saint-martin d'Hères, France

ARTICLE INFO

*Article history:*
Received 28 January 2008
Accepted 6 October 2009

*Keywords:*
Cellulose ethers
Hydration (A)
Adsorption (C)
Dissolution
Nucleation

ABSTRACT

The influence of cellulose ethers (CE) on $C_3S$ hydration processes was examined in order to improve our knowledge of the retarding effect of cellulose ethers on the cement hydration kinetics. In this frame, the impacts of various cellulose ethers on $C_3S$ dissolution, C-S-H nucleation-growth process and portlandite precipitation were investigated. A weak influence of cellulose ethers on the dissolution kinetics of pure $C_3S$ phase was observed. In contrast, a significant decrease of the initial amount of C-S-H nuclei and a strong modification of the growth rate of C-S-H were noticed. A slowing down of the portlandite precipitation was also demonstrated in the case of both cement and $C_3S$ hydration. CE adsorption behavior clearly highlighted a chemical structure dependence as well as a cement phase dependence. Finally, we supported the conclusion that CE adsorption is doubtless responsible for the various retarding effect observed as a function of CE types.



## 1. Introduction

Cellulose ethers (CE) are widespread admixtures introduced into industrial mortar formulations to fulfill specific tasks during the handling stage. As famous thicker and air entrainment agent, CE allow to adjust the workability of the fresh cementitious material at desired level by controlling the water balance. Moreover, CE contribute to reach a high water retention capacity to prevent water from draining out quickly from the mortar to the substrate. Thereby, mechanical, adhesive and water retention properties of mortar were significantly improved in the presence of CE. However, as a side effect, CE may also induce an uncontrolled and problematical retardation of cement hydration.

Nowadays, the knowledge of the molecular parameters that enable to control and to predict the hydration kinetics of cement containing CE was well elucidated [1,2]. The degree of substitution appears as the most relevant structural parameter on the kinetics of cement hydration. Furthermore, other results pointed out that CE seem to have phase-specific retarding effects on cement hydration processes [3,4]. Regarding the stability of CE in alkaline media, it was demonstrated that there was no significant degradation of CE and therefore a negligible impact of hydroxy acids was generated on cement hydration kinetics [5]. In spite of these recent insights on cement–CE interactions, the mechanism at the origin of the hydration delay induced by CE remains not perfectly understood. Because Portland cement is a complex material composed by many reactive phases, any statement concerning the interaction of its mineral phases and organic compounds must be made carefully. In this sense, we choose to focus on the cellulose ether interactions with tricalcium silicate ($C_3S$), the main phase of Portland cement. Consequently, the influence of CE on $C_3S$ dissolution, and their impact on C-S-H nucleation-growth processes as well as portlandite (CH) precipitation are investigated and discussed in the present study.

Moreover, the current understanding of the mechanism of polysaccharide adsorption onto mineral surfaces suggests an acid/base interaction [6–8]. It was generally assumed that polysaccharides interact with metal hydroxylated species that are anchored at the mineral surface. Nevertheless very few papers dealt with CE adsorption on cement phases [9]. In particular, the phase dependence and the structural parameter dependence of cellulose ether adsorption were still not elucidated. That is why, this paper is also devoted to the investigation of CE adsorption behaviors on cementitious phases.

## 2. Mineral and organic compounds

The investigated ordinary Portland cement (OPC) was a CEM I 52.5 R CE CP2 NF type cement according to the EN 197-1 standard. Its chemical and phase compositions are given in Table 1. The $C_3S$ pure phase used for this study was supplied by the Lafarge company (France). X-ray diffraction analysis (Siemens, D 5000) allowed to put in evidence a very low content of free lime (approximately 0.5 wt.%). The C-S-H phase was prepared by the so-called pozzolanic method [10], *i.e.* by reacting lime (heating Aldrich calcium carbonate at 1100 °C for 3 h) with silica fume (Degussa Aerosil 200). To avoid carbonation, the reaction occurs under nitrogen environment. The mixture was kept at 60 °C during 6 months. X-ray diffraction confirmed that pure 14 Å tobermorite-like C-S-H was obtained [11].

* Corresponding author. Tel.: +33 4 77 42 01 80; fax: +33 4 77 49 96 94.
*E-mail address:* pourchez@emse.fr (J. Pourchez).

0008-8846/$ – see front matter © 2009 Elsevier Ltd. All rights reserved.
doi:10.1016/j.cemconres.2009.10.008

**Table 1**
Chemical and phase compositions of the investigated mineral phases.

| BET surface area | | Cement chemical composition (wt.%) | | Cement phase composition (wt.%) | | |
|---|---|---|---|---|---|---|
| Mineral phases | Surface area ($m^2 g^{-1}$) | Oxides | XRF analysis (%) | Phases | XRF analysis and Bogue (%) | XRD analysis and Rietveld (%) |
| Cement | 1.53 ± 0.03 | CaO | 67.1 | $C_3S$ | 67.5 | 69.4 |
| $C_3S$ | 0.92 ± 0.02 | $SiO_2$ | 21.2 | $C_2S$ | 9.8 | 9.3 |
| C-S-H | 23.4 ± 0.35 | $Al_2O_3$ | 4.3 | $C_3A$ | 8.3 | 8.3 |
| CH | 15.2 ± 0.15 | $SO_3$ | 4.6 | $C_4AF$ | 5.5 | 3.1 |
| | | $Fe_2O_3$ | 1.8 | Gypsum | 4.6 | 3.6 |
| | | MgO | 0.6 | $CaCO_3$ | – | 4.9 |
| | | $TiO_2$ | 0.2 | Anhydrite | – | 1.2 |
| | | $P_2O_5$ | 0.2 | Quartz | – | 0.2 |
| | | $Na_2O$ | 0.2 | | | |
| | | $K_2O$ | 0.1 | | | |

A Ca/Si ratio of the C-S-H phase equal to 1 was characterized by a Bruker-AXS SRS3400 X-ray fluorescence spectroscopy. Finally, the CH phase used was purchased from Merck.

The surface area of the mineral phases was analyzed by nitrogen adsorption in a Micromeritics ASAP 2000 nitrogen adsorption apparatus. The samples measured were degassed at 100 °C before the measurements. The surface area was determined by the multi-point BET method using the adsorption data. Results are reported in Table 1.

Three different HEC molecules (noted H1, N1 and N7) and two HPMCs (named U2 and P1) were selected. Beforehand, a precise characterization was performed (Table 2) by size exclusion chromatography and near infra red spectroscopy analysis [1,2]. It allowed to quantify the structure parameters, *e.g.* the weight-average molecular mass ($\overline{M_w}$), the content of hydroxy ethyl groups, hydroxy propyl groups and methoxyl groups.

## 3. Experimental methods of investigation

### 3.1. Impact of CE on $C_3S$ dissolution

Conductometry is a powerful tool for monitoring the hydration kinetics [1,2,9,12]. The dissolution kinetics of $C_3S$ is monitored by conductometry, in dynamic nitrogen environment to prevent carbonation. To avoid reaching the critical supersaturation with respect to C-S-H and consequently its precipitation, the dissolution tests were performed with a high liquid to solid ratio (L/S), equal to 5000 or 130000 [13,14]. To exhibit the mechanisms controlling the kinetics of $C_3S$ hydration in the presence of CE, we used an experimental approach using conductivity measurement in diluted media previously developed in [15]. Based on this methodology, delayed additions of water, $C_3S$ and C-S-H have been performed to assess the effect of CE on the competition between $C_3S$ dissolution and C-S-H nucleation.

### 3.2. Impact of CE on C-S-H nucleation

The quantity of C-S-H nuclei precipitated at the beginning of the $C_3S$ hydration appears as a useful data to evaluate the impact of CE on the nucleation of C-S-H. By following the evolution of silicate and calcium concentration versus the time of $C_3S$ hydration, the number of initial nuclei of C-S-H is calculated using the gap of silicate concentration during the period where the calcium concentration is still constant [16]. The determination of silicate and calcium concentration was obtained using ionic chromatography. This was performed on a Dionex apparatus composed of a GP50 pump, a CS12A column for cation analysis, a AS11HC column for anions, a CD conductometric detector and an UV-visible detector. The analysis conditions are given in [14].

**Table 2**
Molecular parameters of cellulose ethers.

| Admixtures | $M_w$ (Da) | $OC_2H_4OH$ (%) | $OC_3H_6OH$ (%) | $OCH_3$ (%) |
|---|---|---|---|---|
| HPMC U2 | 955000 | – | 10.65 | 27.5 |
| HPMC P1 | 175000 | – | 19 | 27.5 |
| HEC H1 | 175000 | 48.5 | – | – |
| HEC N1 | 175000 | 56 | – | – |
| HEC N7 | 1335000 | 56 | – | – |

### 3.3. Impact of CE on C-S-H growth

The mechanism of C-S-H formation was previously elucidated by Garrault [16–18]. It occurs *via* a nucleation-growth process. Based on this theory, conductometry in various limewater concentrations appears as a powerful tool to monitor the different kinetic stage of the C-S-H growth (Fig. 1). In this frame the duration changes of the kinetic period, limited by the free growth of C-S-H or by the diffusion through the C-S-H shell around $C_3S$ grain, allow to highlight the impact of CE on the growth rate of C-S-H perpendicular or parallel to $C_3S$ surface.

### 3.4. Impact of CE on CH precipitation

The influence of CE on CH precipitation was examined by conductometry. Experiments were performed in limewater suspension with a liquid to solid ratio (L/S) equal to 20, and a polymer to solid (P/S) weight ratio of 2%. The experiments were thermostated at 25 °C and carried out in triplicate. The initial CH precipitation was represented by an electrical conductivity drop [1,2,19,20]. So, the impact of cellulose ethers on the beginning of CH massive precipitation was determined using time of the conductivity drop as a global kinetic benchmark of silicate phase hydration.

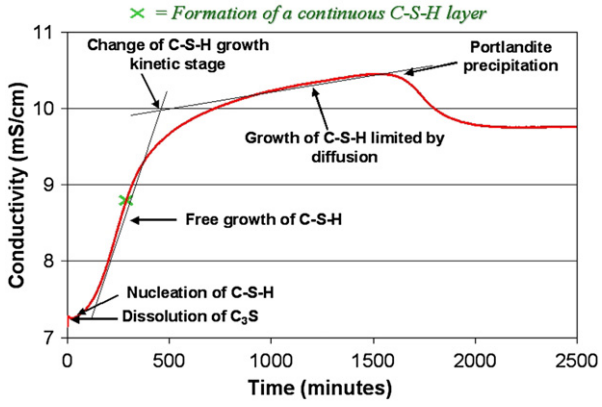


**Fig. 1.** Different steps of the $C_3S$ hydration process in limewater (L/S = 160, P/S = 2%, $[Ca(OH)_2]$ = 20 mM).

### 3.5. Adsorption of CE on mineral phases

The protocol developed was based on the quantitative determination of CE by a phenol-sulfuric acid method. The concept consists of determining the absorbance at 490 nm with a UV-visible spectrophotometer [21]. We put in contact a given CE concentration with a well-characterized mineral phase. After 2 h of exposure time under nitrogen atmosphere and constant magnetic stirring, the suspension was centrifuged. Then, the CE concentration in the supernatant was determined using the phenol-sulfuric acid method. The amount of polymer adsorbed on the mineral phase was easily calculated from the initial well-known CE concentration and the final CE concentration was measured in the supernatant by spectroscopy.

The adsorption of CE on mineral phases was under "stable" conditions (for the hydrated phases) or under "dynamic" conditions (for the anhydrous phases). Under stable conditions, we assume that the hydrated pure phases were in quite stable equilibrium with the liquid phase. In this sense, in order to limit as far as we can any solid dissolution, adsorption experiments were performed with $Ca(OH)_2$-saturated solution previously ion-saturated in respect of each mineral phase investigated. CE were always previously dissolved in the ion-saturated solution prior to the adsorption measurement.

In contrast, under dynamic conditions the hydration process took place during the experiments. The experiments under dynamic conditions lead only to qualitative and comparative statement on CE adsorption. It allows a time-resolved monitoring of CE adsorption during hydration, *i.e.* to follow the CE consumption over the hydration time. CE degradation is considered as negligible during the exposure time [5,22].

## 4. Results

### 4.1. CE adsorption behaviors under stable conditions

The results (Fig. 2) exhibit that a variable amount of CE can be adsorbed on C-S-H (between 0 $mg\,g^{-1}$ for P1, 9.4 $mg\,g^{-1}$ or 400 $\mu g\,m^{-2}$ for H1) and CH (between 5.5 $mg\,g^{-1}$ or 365 $\mu g\,m^{-2}$ for P1, 9.7 $mg\,g^{-1}$ or 635 $\mu g\,m^{-2}$ for H1). The order of magnitude obtained is perfectly in accordance with CE adsorption on CH around 500 $\mu g\,m^{-2}$ measured by Mueller in [4]. We notice that this adsorption mainly depends of the CE-type. As a general rule, the adsorption capacity on C-S-H and CH is higher for HECs (H1, N1 and N7) rather than for HPMCs (U2 and P1). Moreover, in the same CE family, the adsorption is clearly sensitive to the content of substitution groups. Actually, despite the fact that U2 and P1 are two HPMC molecules, the adsorption behavior observed is very disparate. In particular, U2 and P1, varying only by the percentage of hydroxypropyl group variation, show that the lower the content of hydroxypropyl group, the stronger the CE adsorption on C-S-H and CH. The relative impact on the adsorption capacity of the content of hydroxyethyl group is put in evidence in the case of HECs. HEC molecules H1 and N1 (with varying percentages of hydroxyethyl group and identical molecular mass) lead to show again that the lower the content of hydroxyethyl group, the stronger the CE adsorption on C-S-H and CH.

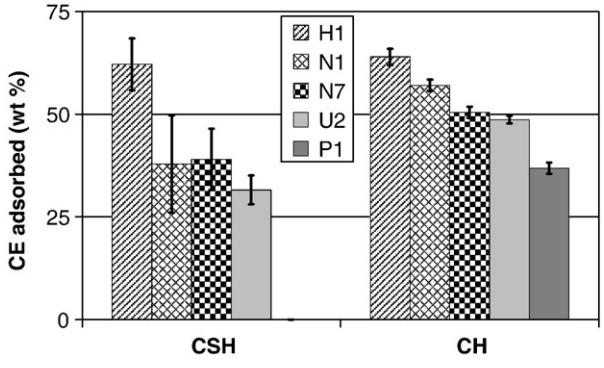


**Fig. 2.** CE adsorption on C-S-H and CH expressed in wt.% after a 2 hour-exposure time (initial concentration of CE equal to 15 mg per g of pure mineral phase introduced, L/S = 20).

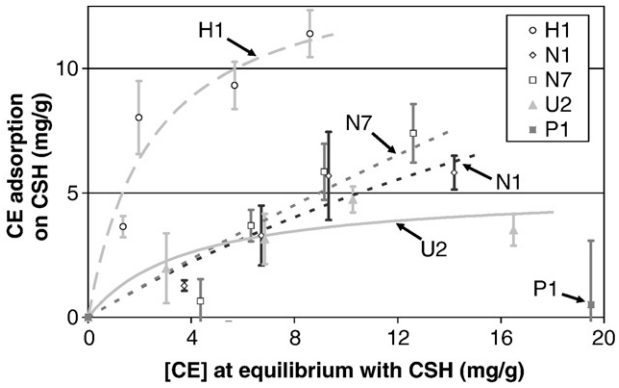


**Fig. 3.** CE adsorption isotherms on C-S-H after a 2 hour-exposure time (L/S = 20).

The polymer to mineral weight ratio was varied so as to establish adsorption isotherms. Results on C-S-H and CH single phases were respectively reported in Figs. 3 and 4. The data was satisfactorily fitted by means of a Langmuir law. The adsorption isotherms lead to establish the relative affinity of the polymer for the mineral phase as well as the amount of polymer adsorbed at the plateau value. Indeed, the higher the slope of the initial linear part of the adsorption isotherm curve, the stronger the polymer relative affinity with the mineral phase. The global tendency observed is a great impact of the CE chemical structure on the relative affinity: the lower the content of hydroxyethyl group (case of HECs H1 and N1) or hydroxypropyl group (case of HPMCs U2 and P1), the higher the relative affinity on C-S-H and CH. Moreover, the relative affinity of CE is clearly higher on CH rather than on C-S-H.

### 4.2. CE adsorption behaviors under dynamic conditions

Whatever the CE studied, the dynamic experiments showed that the CE adsorption on cement phases increased with increasing hydration time (Fig. 5). Furthermore, we perfectly observed that the amount of CE introduced initially is totally consumed after several hours of hydration (in the range 24–48 h). During the first hour of hydration, we suggest that the $C_3S$–water interface is slightly modified, since the variation of specific surface and the amount of C-S-H precipitated is relatively small. Thus, even if the system is never in the thermodynamic equilibrium, we perform "adsorption pseudo-isotherm" using the usual "stable conditions" methodology but with a shorter exposure time (only 1 h). Regarding the standard deviation,

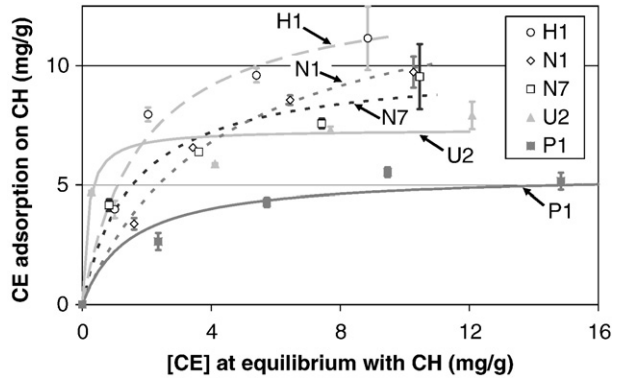


**Fig. 4.** CE adsorption isotherms on CH after a 2 hour-exposure time (L/S = 20).

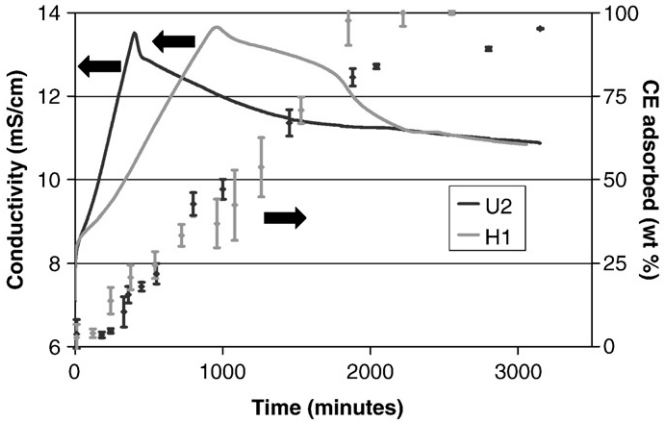


**Fig. 5.** CE consumption during cement hydration followed by conductometry (initial concentration of CE equal to 1 g $L^{-1}$, P/C = 2%, L/S = 20).

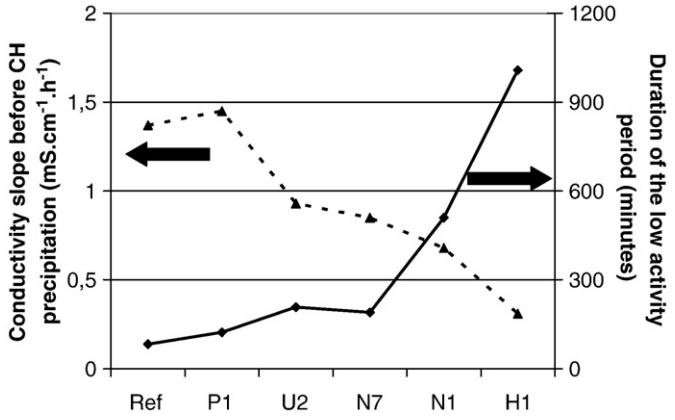


**Fig. 8.** Impact of 5 cellulose ethers on the linear part of the conductivity slope measured before the CH massive precipitation, and the duration of the low activity period, during $C_3S$ hydration (L/S = 20, P/S = 2%, $[Ca(OH)_2]$ = 20 mM, Ref = $C_3S$ phase without CE).

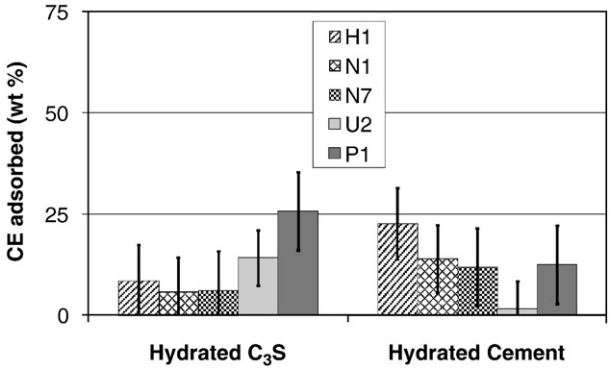


**Fig. 6.** CE adsorption on $C_3S$ and cement after a 1 hour-exposure time (initial concentration of CE equal to 15 mg per g of anhydrous phase introduced initially, L/S = 20).

the adsorption pseudo-isotherm behavior observed on hydrated cement and hydrated $C_3S$ single phases (Fig. 6) is quite low compared to the amount of CE adsorbed on hydration products such as C-S-H and CH (Fig. 2). This result is correlated with the very low CE adsorption measured during the first hour of cement hydration under dynamic conditions (Fig. 5). These results showed a possible but quite low adsorption capacity of CE on anhydrous phases.

### 4.3. Influence of CE on $C_3S$ dissolution: qualitative approach

When the $C_3S$ hydration occurs, a more or less important duration of the low activity period (*e.g.* a conductivity plateau) can be observed as a function of the chemical nature of the CE introduced (Figs. 7 and 8). According to the experimental results on Figs. 7 and 8, it appears obvious that the $C_3S$ dissolution rate can be very low in the presence of CE. Our investigations focused on the understanding of the duration change of the period where the aqueous concentration remains quite constant in the presence of CE (Fig. 8).

At first, some water is added during the conductivity plateau of $C_3S$ hydration in water diluted media admixed with the HEC named H1 (Fig. 9). The water delayed addition is equal to 30 wt.% of the amount of water initially introduced. H1 was chosen since this molecule has the stronger $C_3S$ hydration slowing down capacity (Fig. 8). A rapid drop of conductivity is initially noticed owing to the dilution effect. Then, an increase of conductivity is obvious due to the rise of $C_3S$ dissolution in order to compensate the dilution effect induced by water addition. Finally, the conductivity attained the same value observed just before water addition. Nevertheless, we can notice that a few minutes after the delayed addition of water, a much lower conductivity value is observed compared with the reference curve without water addition. This can be easily explained due to the change of liquid to solid ratio induced by the delayed addition of water [15]. Therefore, we propose that $C_3S$ dissolution in the presence of CE is certainly not directly blocked during the important duration of the low activity period. In fact, the composition of the liquid phase during this period seems to be mainly limited by the critical supersaturation level reached with respect to C-S-H (*i.e.* the composition of the aqueous phase corresponding to the conductivity plateau). As water addition do not modify the critical supersaturation level attained with respect to C-S-H, the same limit of liquid phase composition (*i.e.*

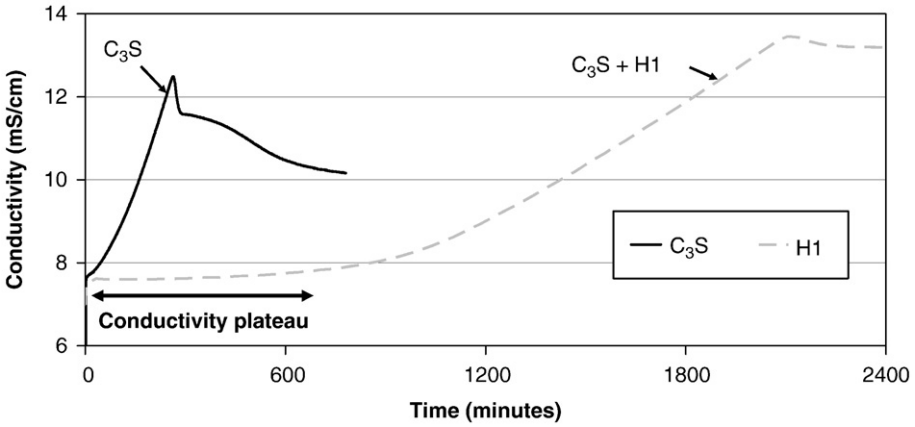


**Fig. 7.** Impact of HEC H1 on the duration of the conductivity plateau during $C_3S$ hydration in limewater suspension (L/S = 20, P/S = 2%, $[Ca(OH)_2]$ = 20 mM).

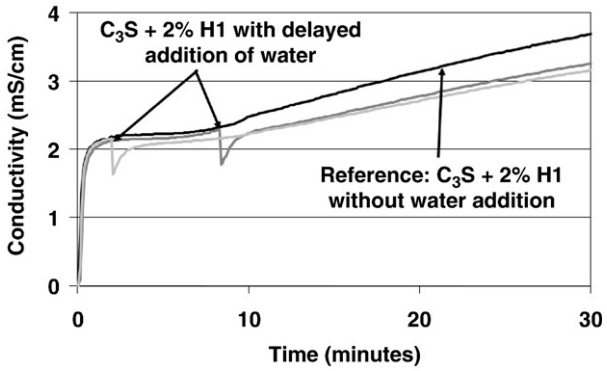


**Fig. 9.** Delayed addition of water during the conductivity plateau at the beginning of the $C_3S$ hydration in water suspension with H1 (L/S = 70, P/S = 2%). The water delayed addition corresponds to 30 wt.% of the amount of water initially introduced.

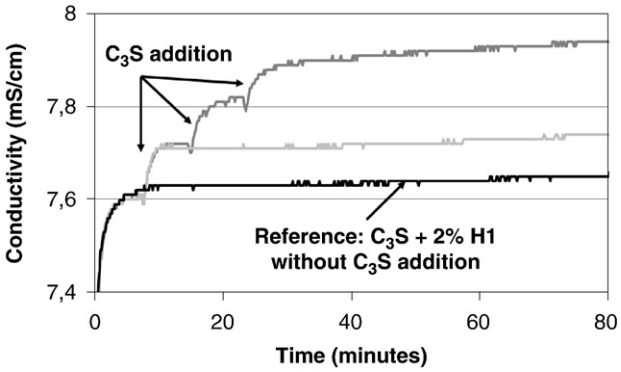


**Fig. 11.** Delayed addition of $C_3S$ during the conductivity plateau at the beginning of the $C_3S$ hydration in limewater suspension with H1 (L/S = 40, P/S = 2%). The $C_3S$ delayed addition corresponds to 30 wt.% of the amount of $C_3S$ initially introduced.

the same conductivity value at the plateau) is observed after water addition.

In contrast, C-S-H addition decreases the critical supersaturation reached with respect to C-S-H. The C-S-H delayed addition corresponds to 30 wt.% of the amount of $C_3S$ initially introduced. During the hydration process, the critical supersaturation level with respect to a hydrate decreases as precipitation creates more and more seeds. Consequently, by a seeding effect, C-S-H addition induced a rapid drop of conductivity corresponding to a massive precipitation of C-S-H from the calcium and silicate ions accumulated in the solution (Fig. 10). Then, the conductivity increases and the period of limitation of the aqueous concentration (*i.e.* the conductivity plateau) is not observed again.

The last delayed addition experiments consist of $C_3S$ addition during the conductivity plateau. The $C_3S$ delayed addition corresponds to 30 wt.% of the amount of $C_3S$ initially introduced. So, if $C_3S$ is added during the conductivity plateau in the presence of H1, a new conductivity plateau is noticed but at a higher conductivity value (Fig. 11). This process is repeated several times and a conductivity curve with several steps is finally observed. The $C_3S$ addition leads to increase the critical supersaturation level reached with respect to C-S-H. The rise of conductivity just after $C_3S$ addition shows that the $C_3S$ added is dissolved.

Our results performed in CE admixed system are perfectly similar to the experiments of $C_3S$, C-S-H and water delayed addition previously carried out in non admixed system by Damidot et al. [15]. Based on these data, we can suggest that $C_3S$ dissolution is certainly not directly blocked by CE, but rather limited by the ionic composition of the liquid phase induced by CE.

### 4.4. Influence of CE on $C_3S$ dissolution: quantitative approach

The kinetics of $C_3S$ dissolution in the presence of CE were examined. The precipitation of C-S-H does not consume all the calcium and hydroxide ions released during the $C_3S$ dissolution. Thus, neglecting the impact of the very low CE concentration on the electrical conductivity (this assumption was successively verified), as long as the precipitation of CH was not started, the electrical conductivity of the solution is directly proportional to the calcium concentration [23]. Under very high diluted media (L/S higher than 100000), we prefer to follow the silicate concentration by ionic chromatography in order to calculate the $C_3S$ dissolution advancement.

Firstly, the $C_3S$ dissolution kinetics experiments were conducted in very high water diluted media (L/S = 5000), in argon environment, to avoid any precipitation (and in particular C-S-H precipitation). Thus the $C_3S$ is quickly and totally dissolved, and the liquid phase never reaches the critical supersaturation with respect to C-S-H. The impact of CE on $C_3S$ dissolution kinetics (Fig. 12) emphasizes that the admixtures do not appear to modify the dissolution kinetics of $C_3S$. The slopes of the curves (calculated by regression in origin) corresponding to the initial dissolution rate are rigorously identical regardless of the chemical nature of the CE introduced.

However, the calcium hydroxide concentration is a key parameter controlling the dissolution kinetics of $C_3S$. The huge role it plays on the rate of solid–liquid reactions by the gap from the thermodynamic solubility equilibrium of dissolved solid is well-known [24]. Therefore, the saturation index has a great impact on the mechanisms involved in kinetic dissolution: the higher the undersaturation of a mineral, the faster its dissolution. Thus, in very high limewater diluted media, the

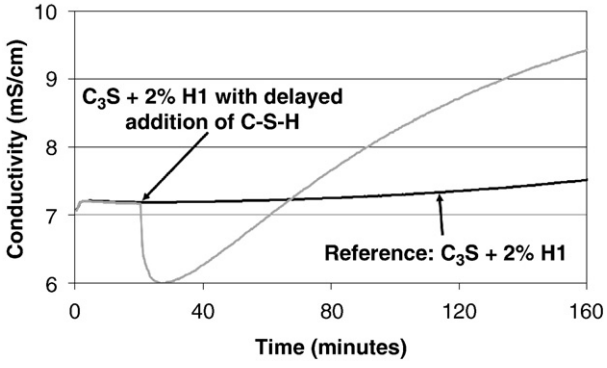


**Fig. 10.** Delayed addition of C-S-H during the conductivity plateau at the beginning of the $C_3S$ hydration in limewater suspension with H1 (L/S = 160, P/S = 2%). The C-S-H delayed addition corresponds to 30 wt.% of the amount of $C_3S$ initially introduced.

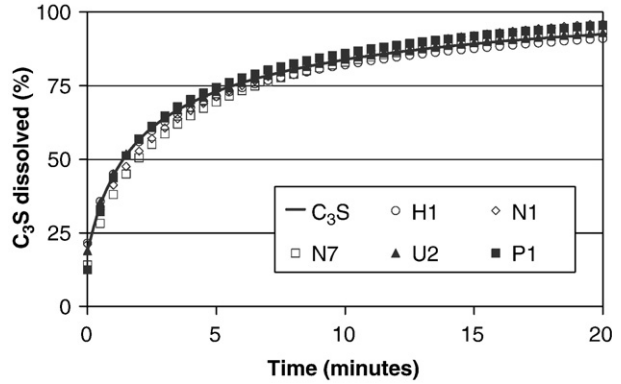


**Fig. 12.** Impact of cellulose ethers on the $C_3S$ dissolution kinetics in water diluted media (L/S = 5000, [CE] = 1 g $L^{-1}$).

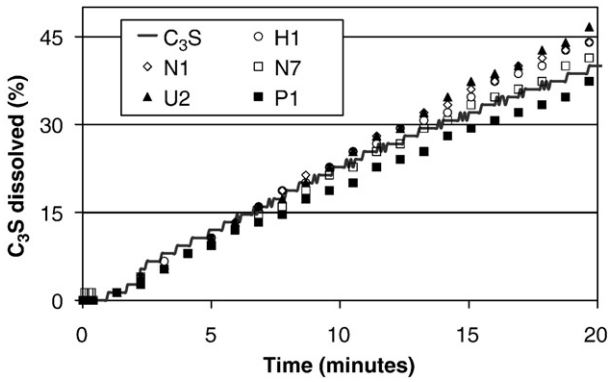


**Fig. 13.** Impact of cellulose ethers on the $C_3S$ dissolution kinetics in limewater diluted media ($[Ca(OH)_2] = 10$ mM, L/S = 130000, $[CE] = 1\ g\,L^{-1}$).

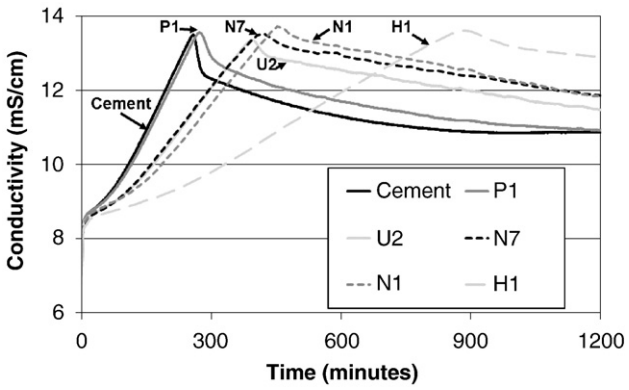


**Fig. 15.** Impact of CE on the cement hydration behavior monitored by conductometry measurement in limewater suspension under argon atmosphere (L/S = 20, P/S = 2%, $[Ca(OH)_2] = 20$ mM).

initial $C_3S$ dissolution rate strongly slows down rather than in very high water diluted media. Based on this knowledge, some authors perfectly demonstrate that some latexes exhibit a more or less $C_3S$ dissolution inhibition [25]. The monitoring of $C_3S$ dissolution phenomena emphasizes insignificant influence of CE (Fig. 13). As a matter of fact, the slopes of the curves corresponding to the initial dissolution rate are similar regardless of the chemical nature of CE ($2.3 \pm 0.15$ wt.%$\,min^{-1}$). We should also notice that the polymer to $C_3S$ ratio is very high (around 130). Thus, if the CE can inhibit $C_3S$ dissolution in the case of a polymer to $C_3S$ ratio equal to 2% (the ratio where we observe a very important duration of the low activity period!), a strong effect should be observed with a polymer to $C_3S$ ratio equal to 130. By way of conclusion, the results obtained indicate a quite low impact of CE on $C_3S$ dissolution kinetics as a global tendency.

### 4.5. CE action on C-S-H and CH precipitation

Conductivity measurement of cement and $C_3S$ admixed suspensions were successively performed (Figs. 14 and 15). We observed, whatever the $C_3S$ or cement hydration, a CE-type impact on the hydration kinetic with a gradual delay in the following order: from the highest slowing down induced by H1, to the lowest slowing down induced by P1. Moreover, the conductivity experiments exhibit clearly that CE can cause a more or less important conductivity plateau at the beginning of the $C_3S$ hydration (Fig. 14). It means that CE act during the period of $C_3S$ hydration when the competition between the $C_3S$ rate of dissolution and the C-S-H rate of precipitation occurs.

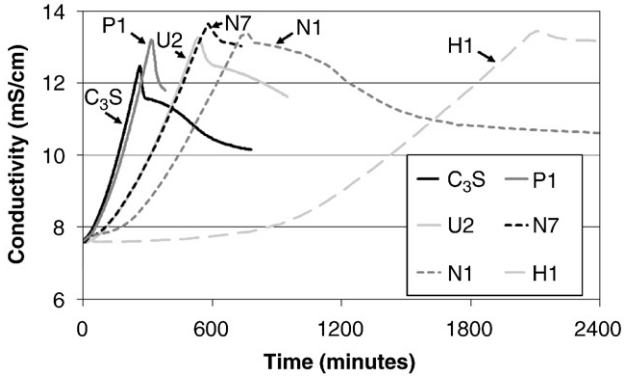


**Fig. 14.** Impact of CE on the $C_3S$ hydration behavior monitored by conductometry measurement in limewater suspension under argon atmosphere (L/S = 20, P/S = 2%, $[Ca(OH)_2] = 20$ mM).

### 4.6. Impact of CE on C-S-H nucleation

Results reported in Fig. 16 show that CE lead to decrease the initial amount of C-S-H seeds. Thus, CE seem to slow down the heterogeneous nucleation of C-S-H on the surface of $C_3S$ grains. The kinetics initial stage of $C_3S$ hydration may be explained by only considering the nucleation and growth of clusters of C-S-H on the $C_3S$ surface [17]. In this sense, the decrease of the quantity of C-S-H nucleating during the beginning of $C_3S$ hydration can strongly contribute to the increase of the duration of the conductivity plateau in the presence of CE. This assumption appears coherent with the results described in this paper since we notice that the higher the inhibition capacity of C-S-H nucleation, the longer the duration of the low activity period (*i.e.* the conductivity plateau).

### 4.7. Impact of CE on C-S-H growth

The proposed approach consists of monitoring the duration changes of the kinetic period limited by the free growth of C-S-H or by the diffusion through the C-S-H shell around the $C_3S$ grain. In this frame, we used the time of change of C-S-H growth kinetic stage (easily determined on the conductometric curves — see Fig. 1) as a useful benchmark to highlight the impact of CE on the growth rate of C-S-H [26,27].

The $C_3S$ hydration in a 20 mM limewater media was firstly examined. All CE show the same behavior (whatever the concentration of limewater), even if the tendencies were always exacerbated for the molecule H1. That is why, only the results for H1 are reported in Figs. 17 and 18. The higher the amount of CE introduced, the higher

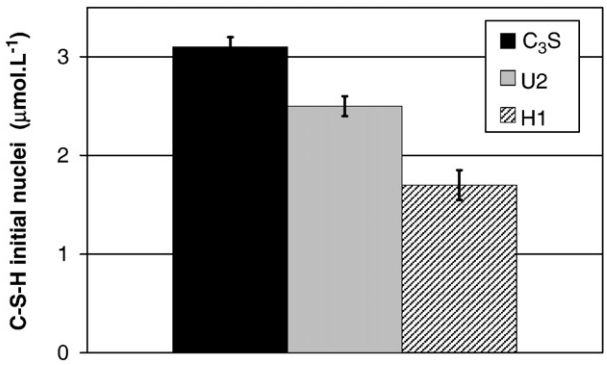


**Fig. 16.** Impact of CE on the amount of initial nuclei of C-S-H precipitated after 30 min of $C_3S$ hydration (L/S = 100, P/S = 2%, $[Ca(OH)_2] = 20$ mM, volume of 100 mL).

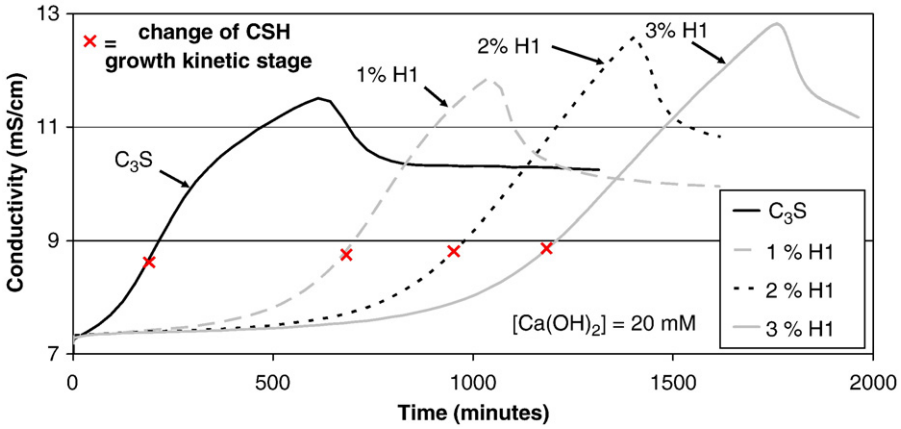


**Fig. 17.** Conductometric curves of $C_3S$ hydration admixed with various amount of H1 (L/S = 100, $[Ca(OH)_2]$ = 20 mM).

the retardation of CH precipitation, and in the same time the higher the conductivity value reached when CH massive precipitation begins (*i.e.* the higher the critical supersaturation reached with respect to CH). Moreover, common behaviors on C-S-H growth process are observed:

- ➢ The higher the amount of CE added, the higher the conductivity value when the change of C-S-H growth kinetic stage occurs (*i.e.* the higher the thickness of the C-S-H layer at the time corresponding to the formation of a C-S-H shell around the $C_3S$ grain).
- ➢ The change of C-S-H growth kinetic stage is delayed when the amount of CE increases. Thus, in the presence of CE, we emphasize that, the duration of the kinetic period limited by the free growth of C-S-H increases, and the $C_3S$ hydration time when the kinetic period limited by the diffusion through the C-S-H shell around the $C_3S$ grain is delayed.

However, concentration of limewater is a well-known parameter which plays a major role on the rates of C-S-H growth [26,27]. As a result, in order to evaluate the possible action of CE on the C-S-H growth rates, we also examine the case of $C_3S$ hydration in a 15 mM limewater media. As discussed above, only the results for H1 are reported in Figs. 19 and 20. In this specific hydration conditions, CE accelerate the beginning of CH massive precipitation (*i.e.* the higher the amount of CE, the earlier the CH massive precipitation begins). We emphasized also that the higher the amount of CE, the higher the critical supersaturation with respect to CH massive precipitation. Finally, specific impacts of CE on the C-S-H growth were noticed:

- ➢ CE delay the formation of a continuous C-S-H layer around the $C_3S$ grain because the time of change of C-S-H growth kinetic stage that appears much later as the amount of CE introduced is important.
- ➢ CE increase the conductivity value reached when the change of C-S-H growth kinetic stage occurs.
- ➢ CE can modify the permeability of the C-S-H shell around the $C_3S$ grain, since the duration of the C-S-H growth kinetic stage limited by the diffusion of ionic species through the C-S-H layer decreases and the slope of the conductivity curve during this period increases.

To sum up, whatever the limewater media, results highlight a same global effect of CE on the C-S-H growth process. At first, the formation of the C-S-H shell around $C_3S$ grain is delayed in the presence of CE. Moreover, when the continuous C-S-H layer appears, the C-S-H layer seems to be a thicker and more permeable and porous barrier compared to the C-S-H shell formation in the case of non admixed $C_3S$ hydration (Fig. 21).

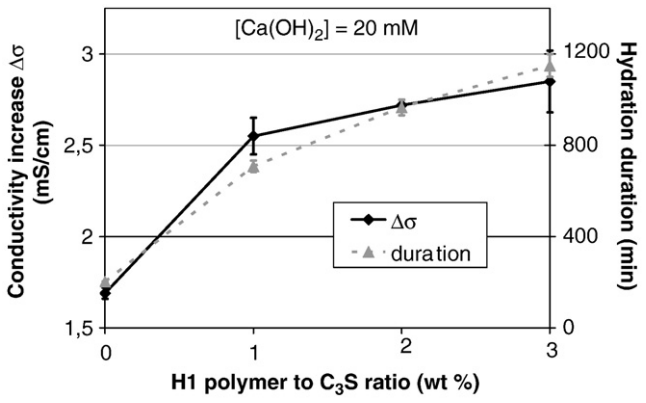


**Fig. 18.** Characteristics of the C-S-H growth kinetic stage (conductivity increase at the change of C-S-H growth kinetic stage, and hydration duration to attain the change of C-S-H growth kinetic stage) during $C_3S$ hydration admixed with various amount of H1 (L/S = 100, $[Ca(OH)_2]$ = 20 mM).

## 5. Discussion

We highlighted that CE is totally consumed after several hours of cement hydration (Fig. 5). Two different mechanisms can explain this CE consumption over the hydration time: the steadily increasing of the surface area (due to the continuous precipitation of hydration products) accessible to CE adsorption, and/or the incorporation as an inclusion during the growth process of the CE-molecule adsorbed on the surface of a growing hydrate. Moreover, CE has a strong affinity for aluminate phases [9]. As a result, we must bear in mind that data on cement hydration don't reflect only the $C_3S$-CE interactions.

Comparing the adsorption behavior (Fig. 2) and the hydration delay on CH massive precipitation induced by each CE-molecules (Fig. 14), it appears that the longer the conductivity plateau at the beginning of the admixed $C_3S$ hydration, the higher the amount of CE adsorbed on pure C-S-H phase. For example, the molecule named P1, which is not adsorbed on C-S-H, exhibits a similar kinetic hydration behavior to the reference. On the contrary, the molecule named H1, with a huge adsorption capacity of 62 wt.% on C-S-H, induces a very important conductivity plateau around an 800 minute duration. As a result, we propose that the influence observed on the C-S-H precipitation rate mainly depends on the adsorption capacity of CE on C-S-H. More generally, we notice that the higher the CE adsorption capacity on C-S-H and CH (Fig. 2), the stronger the retardation on silicate hydration (Figs. 14 and 15).

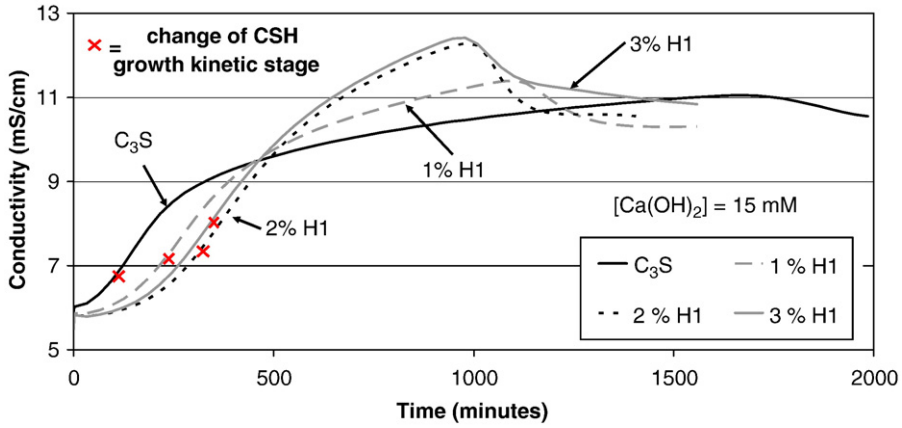


**Fig. 19.** Conductometric curves of $C_3S$ hydration admixed with various amount of H1 (L/S = 100, $[Ca(OH)_2]$ = 20 mM).

Moreover, the results of CE impact on C-S-H growth let us think that CE could retard the formation of a C-S-H shell around the $C_3S$ grain. Several explanations may be proposed to explain this behavior: (i) an inhibition of C-S-H nucleation, (ii) a slowing down of the growth rate of C-S-H parallel to $C_3S$ surface with no significant change of the growth rate of C-S-H perpendicular to $C_3S$ surface, (iii) a slowing down of both the growth rate of C-S-H parallel and perpendicular to $C_3S$ surface. All things considered, it seems that CE could modify the balance between the rates of C-S-H growth parallel or perpendicular to $C_3S$ surface. More precisely, it seems that CE could act preferentially in order to decrease the C-S-H growth parallel to $C_3S$ surface. Consequently, if we consider that the C-S-H growth proceeds by agglomeration of nanometric thin elements [16–18], we propose that the CE adsorption on C-S-H modifies the mode of the C-S-H particle agglomeration, and then the thickness and porous structure of the C-S-H shell. This influence of CE on the characteristics of the C-S-H shell can be quite similar of the impact yet observed by other authors when a change of lime concentration [16–18] or temperature [28] occurs.

The influence of CE on CH massive precipitation seems also very sensitive to the limewater concentration (Figs. 17 and 19). We assume that CE could modify the porous structure of the C-S-H layer as well as the kinetic characteristics of C-S-H nucleation-growth. These changes induce contrary effects on the beginning of CH massive precipitation. In the case of a 20 mM $Ca(OH)_2$ hydration, the impact of CE on the inhibition of C-S-H nucleation is more important than the changes of the C-S-H shell. As a result, CE delay CH massive precipitation under these conditions. In the case of a 15 mM $Ca(OH)_2$ hydration, the influence of CE on the increase of the C-S-H layer permeability is more important than the inhibition of C-S-H nucleation. As a result, CE accelerate CH massive precipitation under these conditions.

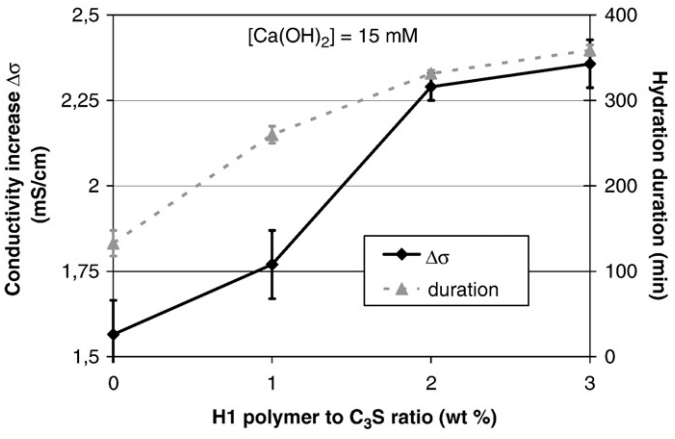


**Fig. 20.** Characteristics of the C-S-H growth kinetic stage (conductivity increase at the change of C-S-H growth kinetic stage, and hydration duration to attain the change of C-S-H growth kinetic stage) during $C_3S$ hydration admixed with various amount of H1 (L/S = 100, $[Ca(OH)_2]$ = 15 mM).

## 6. Conclusion

### 6.1. New insight into CE adsorption behavior on silicate phases

CE emphasize a phase-specific adsorption behavior with a degree of substitution dependence. We observed a high CE adsorption capacity on hydrated phases such as C-S-H and CH, and a weak CE adsorption capacity on anhydrous phases such as $C_3S$. Moreover, the global tendency observed highlights a significant impact of the CE chemical structure on the CE adsorption capacity. The degree of substitution plays a major role on the CE adsorption compared to the molecular mass. We noticed that the lower the content of hydroxyethyl groups or hydroxypropyl groups, the stronger the relative affinity on C-S-H and CH. Furthermore, thanks to a time-resolved monitoring of CE consumption during cement hydration, we also demonstrate that CE can be totally consumed after several hours of cement hydration in diluted media. Finally, the relation between CE adsorption and retardation is quite obvious: high (respectively moderate) and specific adsorption on C-S-H/CH and a great (respectively moderate) impact on C-S-H/CH precipitation kinetics, no significant adsorption on $C_3S$ and no direct effect on $C_3S$ dissolution kinetics.

### 6.2. New insight into CE impact on $C_3S$ hydration

All signs point to exhibit that the influence of CE on $C_3S$ dissolution kinetic is quite low. On the contrary, CE lead to strongly act on the C-S-H precipitation by means of: a decrease of the amount of initial C-S-H seeds, a delay in order to obtain a C-S-H shell around the $C_3S$ grain, and a formation of a thicker and more permeable C-S-H layer. Moreover, a rise of the critical supersaturation level reached to begin the CH massive precipitation is clearly noticed in the presence of CE. When the hydration conditions are favorable to a slow C-S-H nucleation stage and a short duration of the C-S-H growth kinetic stage limited by the diffusion of ionic species through the C-S-H shell (*i.e.* very high limewater media corresponding to quite similar hydration conditions regardless a cement paste), CE retard the CH massive precipitation. On the contrary, when the hydration conditions are favorable to a fast C-S-H nucleation stage and an important duration of the C-S-H growth kinetic stage limited by the diffusion of

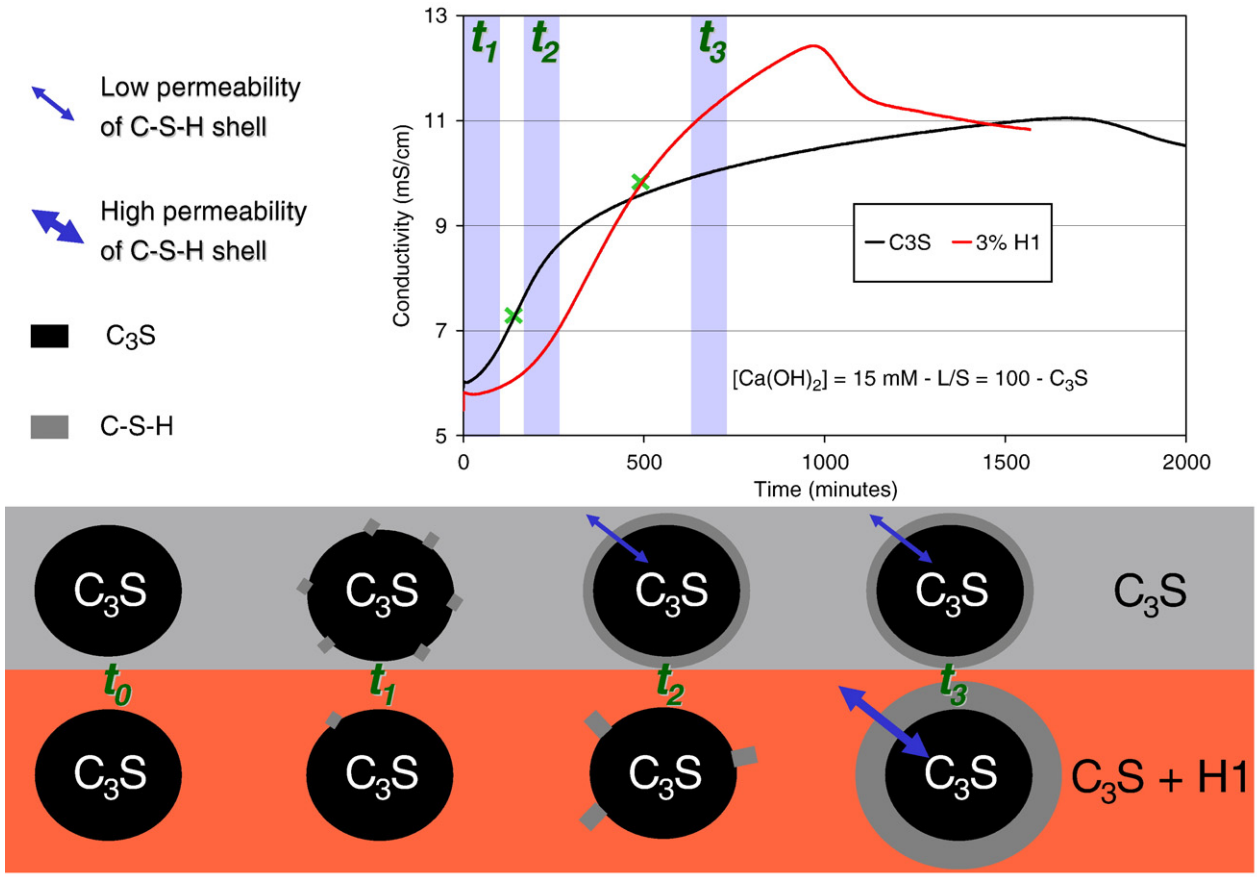


**Fig. 21.** Schematic overview of the cellulose ether impact of the thickness and permeability of the C-S-H shell during $C_3S$ hydration.

ionic species through the C-S-H shell (*i.e.* very low limewater media), CE accelerate the CH massive precipitation.

## Acknowledgements

The authors would like to acknowledge the financial support of the international CEReM network (Consortium for Study and Research on Mortars — http://cerem.cstb.fr), and many helpful conversations with industrial and academic CEReM partners. We also thank Pr. A. Nonat, from the Burgundy University, for the fruitful discussions and comments which have greatly contributed to this paper.

## References

[1] J. Pourchez, A. Peschard, P. Grosseau, B. Guilhot, R. Guyonnet, F. Vallee, HPMC and HEMC influence on cement hydration, Cem. Concr. Res. 36 (2006) 288–294.
[2] J. Pourchez, P. Grosseau, R. Guyonnet, B. Ruot, HEC influence on cement hydration measured by conductometry, Cem. Concr. Res. 36 (2006) 1777–1780.
[3] H.J. Weyer, I. Muller, B. Schmitt, D. Bosbach, A. Putnis, Time-resolved monitoring of cement hydration: influence of cellulose ethers on hydration kinetics, Nucl. Instrum. Methods Phys. Res., B Beam Interact. Mater. Atoms 238 (2005) 102–106.
[4] I. Muller, D. Bosbach, A. Putnis, B. Schmitt, H.J. Weyer, Early hydration processes of Portland cement in presence of cellulose ethers, Procceding of 1 congresso nacional de argamassas de construcao, 2005.
[5] J. Pourchez, A. Govin, P. Grosseau, R. Guyonnet, B. Guilhot, B. Ruot, Alkaline stability of cellulose ethers and impacts of their degradation products on cement hydration, Cem. Concr. Res. 36 (2006) 1252–1256.
[6] Q. Liu, Y. Zhang, J.S. Laskowski, The adsorption of polysaccharides onto mineral surfaces: an acid/base interaction, Int. J. Miner. Process. 60 (2000) 229–245.
[7] J.S. Laskowski, Q. Liu, C.T. O'Connor, Current understanding of the mechanism of polysaccharide adsorption at the mineral/aqueous solution interface, Int. J. Miner. Process. 84 (2007) 59–68.
[8] G. Liu, Q. Feng, L. Ou, Y. Lu, G. Zhang, Adsorption of polysaccharide onto talc, Miner. Eng. 19 (2006) 147–153.
[9] J. Pourchez, P. Grosseau, B. Ruot, Current understanding of cellulose ethers impact on the hydration of $C_3A$ and $C_3A$-sulphate systems, Cem. Concr. Res. 39 (2009) 664–669.
[10] F. Merlin, H. Guitouni, H. Mouhoubi, S. Mariot, F. Vallee, H. Van Damme, Adsorption and heterocoagulation of no ionic surfactants and latex particles on cement hydrates, J. Colloid Interface Sci. 281 (2005) 1–10.
[11] A. Nonat, The structure and stoichiometry of C-S-H, Cem. Concr. Res. 34 (2004) 1521–1528.
[12] A. Nonat, J.C. Mutin, X. Lecocq, S.P. Jiang, Physico-chemical parameters determining hydration and particle interactions during the setting of silicate cements, Solid State Ionics 101–103 (1997) 923–930.
[13] C. Comparet, A. Nonat, S. Pourchet, J.P. Guicquero, E. Gartner, M. Mosquet, Chemical interaction of di-phosphonate terminated monofunctional polyethylene superplasticizer with hydrating tricalcium silicate, Proceeding of the Sixth CANMET/ACI International Conference on Superplasticizers and Other Chemical Admixtures in Concrete, 1997, pp. 61–74.
[14] A. Peschard, A. Govin, J. Pourchez, E. Fredon, L. Bertrand, S. Maximillien, B. Guilhot, Effect of polysaccharides on the hydration of cement suspension, J. Eur. Ceram. Soc. 26 (2006) 1439–1445.
[15] D. Damidot, D. Sorrentino, D. Guinot, Factors influencing the nucleation and growth of the hydrates in cementitious systems: an experimental approach, 2nd International RILEM Workshop on Hydration and Setting, 1997, pp. 161–197.
[16] S. Garrault, A. Nonat, Hydrated layer formation on tricalcium and dicalcium silicate surfaces: experimental study and numerical simulations, Langmuir (2001) 8131–8138.
[17] S. Garrault-Gauffinet, A. Nonat, Experimental investigation of calcium silicate hydrate (C-S-H) nucleation, J. Cryst. Growth (1999) 565–574.
[18] S. Garrault, E. Finot, E. Lesniewska, A. Nonat, Study of C-S-H growth on $C_3S$ surface during its early hydration, Mater. Struct. 38 (278) (2005) 435–442.
[19] D. Damidot, A. Nonat, P. Barret, Kinetics of tricalcium silicate hydration in diluted suspensions by microcalorimetric measurements, J. Am. Ceram. Soc. 73 (11) (1990) 3319–3322.
[20] A. Peschard, A. Govin, P. Grosseau, B. Guilhot, R. Guyonnet, Effect of polysaccharides on the hydration of cement paste at early ages, Cem. Concr. Res. 34 (2004) 2153–2158.
[21] G. Cuesta, N. Suarez, M.I. Bessio, et al., Quantitative determination of pneumococcal capsular polysaccharide serotype 14 using a modification of phenol-sulfuric acid method, J. Microbiol. Meth. (2003) 69–73.
[22] I. Muller, Influence of cellulose ethers on the kinetics of early Portland cement hydration, PhD thesis, University of Karlsruhe, ISSN: 1618-2677, 2007.
[23] D. Damidot, A. Nonat, P. Barret, J. Am. Ceram. Soc. 73 (1990) 3319–3322.
[24] A.A. Jeschke, K. Vosbeck, W. Dreybrodt, Surface controlled dissolution rates of gypsum in aqueous solutions exhibit non linear dissolution kinetics, Geochim. Cosmochim. Acta 65 (2001) 27–34.

[25] S. Pourchet, C. Comparet, L. Nicoleau, A. Nonat, Influence of PC superplasticizers on tricalcium silicate hydration, Proceeding of the 12th International Congress on the Chemistry of Cement, Montréal, 2007.
[26] S. Garrault, A. Nonat, Hydrated layer formation on tricalcium and dicalcium silicate surfaces: experimental study and numerical simulations, Langmuir 17 (2001) 8131–8138.
[27] A. Nonat, J.C. Muttin, X. Lecocq, S.P. Jiang, Physico-chemical parameters determining hydration and particle interactions during the setting of silicate cements, Solid State Ionics 101–103 (1997) 923–930.
[28] M. Zajac, S. Garrault, J.P. Korb, A. Nonat, Effect of temperature on the development of C-S-H during early hydration of $C_3S$, Proceeding of the 12th International Congress on the Chemistry of Cement, Montréal, 2007.